Electronic Supplementary Material (ESI) for ChemComm.

Contents

I. Materials

Trihydroxybenzene (Sigma-Aldrich, 99.0%), 2,3,4,5,6-Pentafluorobenzyl bromide (Acros Organics, 95%), caesium carbonate (Acros Organics, 95%), tetrabutylammonium hydroxide (1.0 M in methanol, Sigma-Aldrich), dodecanethiol(Sigma-Aldrich, 98.0%), benzyl mercaptan (Sigma-Aldrich, 99.0%), Poly(ethylene glycol) methyl ether thiol (Mn 2,000, Sigma-Aldrich), 1,4-Benzenedimethanethiol (Sigma-Aldrich, 98%), tetrabutylammonium fluoride (1.0 M in THF, Sigma-Aldrich), 2-Chloro-3-hydroxybenzaldehyde (Sigma-Aldrich, 97%), p-Toluenesulfonic acid monohydrate (Merck, 99%), trimethyl orthoformate (Combi-Blocks, 98%), triethylamine (Ajax, 95%), imidazole (Sigma-Aldrich, 99.5%), tert-butyldimethylsilyl chloride (Combi-Blocks, 98%), trimethyl phosphite (Alfa Aesar, 97%), titan(IV) chloride (Sigma-Aldrich, 99.9%), sodium bicarbonate (Sigma-Aldrich, 99.5%), magnesium sulphate (Merck, 98%), lithium diisopropylamide solution (2.0 M in THF/heptane/ethylbenzene, Sigma-Aldrich) 2-adamantanone (Sigma-Aldrich, 99%), methylene blue (Alfa Aesar, 95%), compressed oxygen (Supagas, 99.5%) were used as received.
N,*N*-dimethylformamide (DMF, Ajax), acetonitrile (ACN, RCI labscan), tetrahydrofuran (THF, Ajax), dichloromethane (DCM, Fisher Scientific), methanol (Ajax), diethyl ether (Ajax), cyclohexane (CH, Ajax) and ethyl acetate (EA, Ajax), were used as solvents. Deuterated solvent such as chloroform-*d* ($CDCl_3$, 99.8%), ACN-d3 (99.8%)) were purchased from Novachem and used as received.

II. Characterisation Methods

Nuclear magnetic resonance spectroscopy (NMR)

NMR spectra were recorded on a Bruker System 600 Ascend LH, equipped with a BBO-Probe (5 mm) with z-gradient (1H: 600.13 MHz, 13C: 150.90 MHz,19F: 564.63 MHz, respectively). Chemical shifts are expressed in parts per million (ppm) relative to tetramethylsilane (TMS) and referenced to characteristic residual ^{1}H solvent resonances as internal standards [$CDCl_3$: 7.26 ppm; ACN-d3: 1.94 ppm; THF-d8: 1.72 ppm]. ^{19}F spectra were referenced *via* the according Ξ values (^{19}F: Ξ = 94.094) based on the corresponding ^{1}H NMR spectrum. ^{1}H and ^{19}F NMR spectra are reported as follows: chemical shift (δ in ppm), multiplicity (s for singlet, d for doublet, t for triplet, q for quartet, p for pentet, m for multiplet,), coupling constant(s) (Hz), number of protons (concluded from the integrals), specific assignment. ^{19}F NMR spectra were subjected to baseline correction *via* a multipoint fit function. ^{13}C-{^{1}H} NMR spectra are reported in terms of chemical shift and specific assignment.

Size Exclusion Chromatography

The SEC measurements were conducted on a PSS SECurity2 system consisting of a PSS SECurity Degasser, PSS SECurity TCC6000 Column Oven (35 °C), PSS SDV Column Set (8x150 mm 5 µm Precolumn, 8x300 mm 5 µm Analytical Columns, 100000 Å, 1000 Å and 100 Å) and an Agilent 1260 Infinity Isocratic Pump, Agilent 1260 Infinity Standard Autosampler, Agilent 1260 Infinity Diode Array and Multiple Wavelength Detector (A: 254 nm, B: 360 nm), Agilent 1260 Infinity Refractive Index Detector (35 °C). HPLC grade THF, stabilized with BHT, is used as eluent at a flow rate of 1 $mL \cdot min^{-1}$. Narrow disperse linear poly(styrene) (Mn: 266 $g \cdot mol^{-1}$ to 2.52x106 $g \cdot mol^{-1}$) and poly(methyl methacrylate) (Mn: 202 $g \cdot mol^{-1}$ to 2.2x106 $g \cdot mol^{-1}$) standards (PSS ReadyCal) were used as calibrants. All samples were passed over 0.22 µm PTFE membrane filters. Molecular weight and dispersity analysis was performed in PSS WinGPC UniChrom software (version 8.2).

Liquid Chromatrography – Mass Spectrometry (LC-MS)

LC-MS measurements were performed on an UltiMate 3000 UHPLC System (Dionex, Sunnyvale, CA, USA) consisting of a pump (LPG 3400SZ), autosampler (WPS 3000TSL) and a temperature-controlled column compartment (TCC 3000). Separation was performed on a C18 HPLC column (Phenomenex Luna 5µm, 100 Å, 250 × 2.0 mm) operating at 40 °C. Water (containing 5 mmol L-1 ammonium acetate) and acetonitrile were used as eluents. A gradient of acetonitrile:H_2O 5:95 to 100:0 (v/v) in 7 min at a flow rate of 0.40 $mL \cdot min^{-1}$ was applied. The flow was split in a 9:1 ratio, where 90 % of the eluent was directed through a DAD UV-detector (VWD 3400, Dionex) and 10 % was infused into the electrospray source. Spectra were recorded on an LTQ Orbitrap Elite mass spectrometer (Thermo Fisher Scientific, San Jose, CA, USA) equipped with a HESI II probe. The instrument was calibrated in the m/z range 74-1822 using premixed calibration solutions (Thermo Scientific). A constant spray voltage of 3.5 kV, a dimensionless sheath gas and a dimensionless auxiliary gas flow rate of 5 and 2 were applied, respectively. The capillary temperature and was set to 300 °C, the S-lens RF level was set to 68, and the aux gas heater temperature was set to 100 °C.

Chemiluminescence (CL) Kinetics

Emission intensities of chemiluminescence was investigated using a Tecan Spark multimode microplate reader. CL measurements were performed using an OptiPlate-96 Black Opaque microplate (Polystyrene, PerkinElmer). The investigated fluoride concentration of the solutions ranged from 1 to 10 mM. The photon count was measured in luminescence mode in 30 s intervals for 15 h in the range of 400 to 650 nm using an integration time of 10 ms (software Tecan SparkControl). At the beginning of each interval, the reader plate was shaken mechanically in a double-orbital to ensure sufficient mixing of the solution. By

adding 50 µL of fluoride solution into each well of the reading plate, down to 5 nmol of fluoride could be detected per well, when using the settings as described above. The procedure is as follows: 50 µL of a fluoride containing sample (1-10mM, either TBAF or PFTR crude mixtures) were added to a well of the reader plate. Subsequently, 50 µL of a 12 mM dioxetane solution in ACN was added to each well, the well plate was covered with an appropriate cover slide and the measurement was started immediately.

The limit of detection (*DL*) under the present instrument settings was determined from the below formula as per user's manual:

$$DL = \frac{n_{fluoride} * 3 * SD_{blank}}{mean_{fluoride} - mean_{blank}} \approx 2 * 10^{-5} mol \triangleq 20\ \mu mol$$

With $n_{fluoride}$ being the moles of fluoride per well, $mean_{fluoride}$ the average CL intensity in cts for samples of the same $n_{fluoride}$, $mean_{blank}$ the average intensity of blank wells in cts and SD_{blank} the standard deviation of the blanks in cts.

It should be noted though that the limit of detection can be further decreased by increasing the integration time from 10 ms to up to 1000 ms. Thus, concentrations of down to $5*10^{-9}$ mol (5 nmol) can be detected and distinguished from blanks.

Photoreactor

The samples were irradiated in a Luzchem LZC-4V photoreactor using LZC-VIS lamps, emitting in the complete visible range (see spectrum below). Ten lamps were installed for side and top irradiation. Homogeneous irradiation was achieved by stirring the sample solutions during irradiation. The internal chamber was ventilated to maintain ambient temperature during the entire experiment.

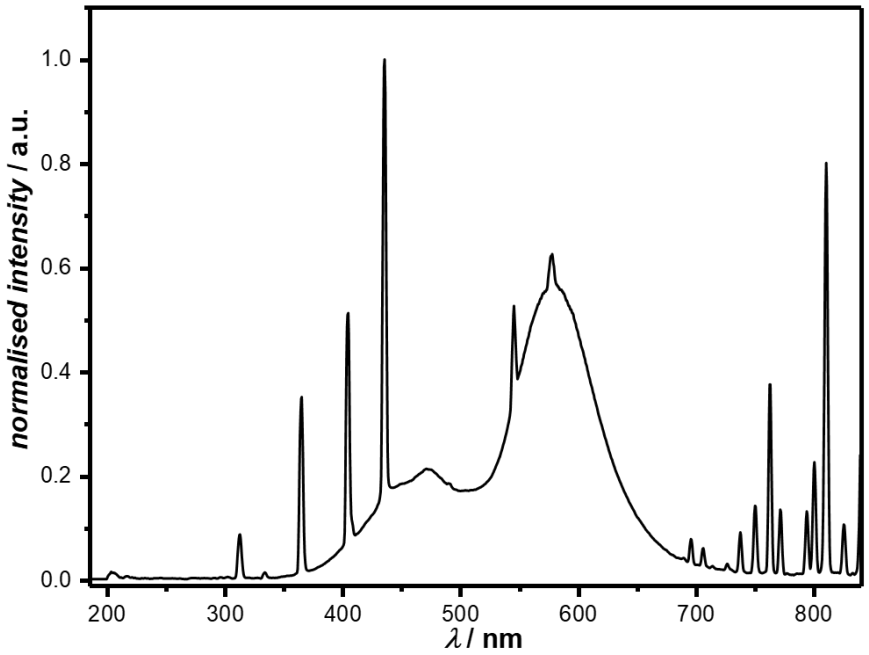

Figure S1. Emission spectrum of the LZC-Vis lamps.

III. Syntheses

1,3,5-Tris(2,3,4,5,6-pentafluorobenzyl) benzene (3PFB)

In a pre-dried Schlenk flask, Cs_2CO_3 (12.9 g, 39.7 mmol, 5.00 eq) was dispersed in dry-DMF (50.0 mL) under argon atmosphere before adding trihydroxybenzene (1.00 g, 7.93 mmol, 1.00 eq). After stirring for 30 min, 2,3,4,5,6-pentafluorobenzyl bromide (3.59 mL, 6.21 g, 23.8 mmol, 3.00 eq) was added and the reaction mixture was stirred for two days at 40 °C. Subsequently, Cs_2CO_3 was filtered off and the filtrate diluted with water (1x 20 mL) and extracted with DCM (2x 20 mL). The collected organic phases were washed with brine (1x 40 mL), dried over magnesium sulphate and concentrated under reduced pressure. The crude product was recrystallised from acetonitrile to give the desired product (1.81 g, 34%).

^{1}H NMR ($CDCl_3$): δ = 5.08 (s, 6H, **CH_2**-O), 6.26 (s, 1H, **CH_{Ar}**) ppm. **^{19}F NMR** ($CDCl_3$): δ = -142.26 (dd, ^3J = 22.2 Hz, 8.6 Hz, 6F, *ortho*), -152.14 (t, ^3J = 20.6 Hz, 3F, *para*), -161.51 (dt, ^3J = J = 21.8 Hz, 8.3 Hz, 6F, *meta*) ppm. **^{13}C NMR** ($CDCl_3$): δ = 160.06 (C_qO), 145.90 (CF), 142.01 (CF), 137.73 (CF), 109.92 ($C_{arom,q}$), 95.60 (CH_{Ar}), 57.64 (CH_2-O) ppm. **HR-ESI-MS**: m/z = 666.0377 ($M+Na^+$, calculated: 666.0312, Δ_{abs} = 0.0065, Δ_{rel} = 9.76 ppm).

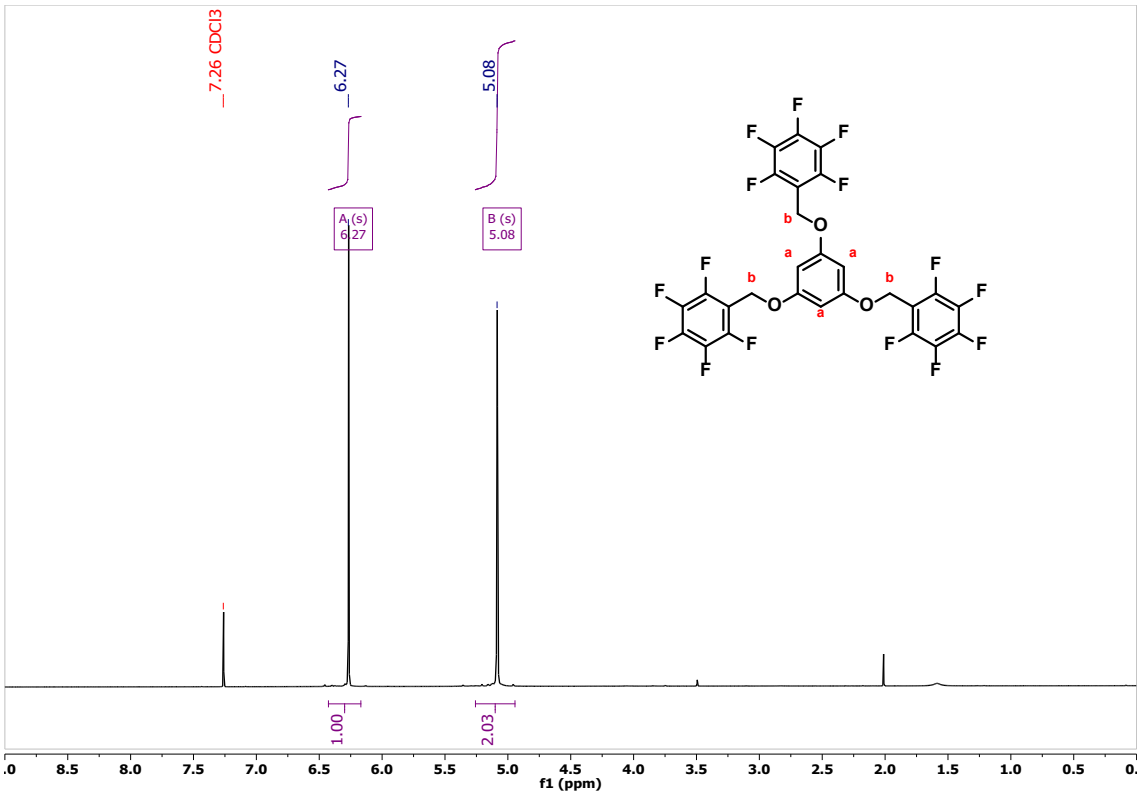

Figure S2. ^{1}H NMR spectrum ($CDCl_3$, 600 MHz) of **3PFB**.

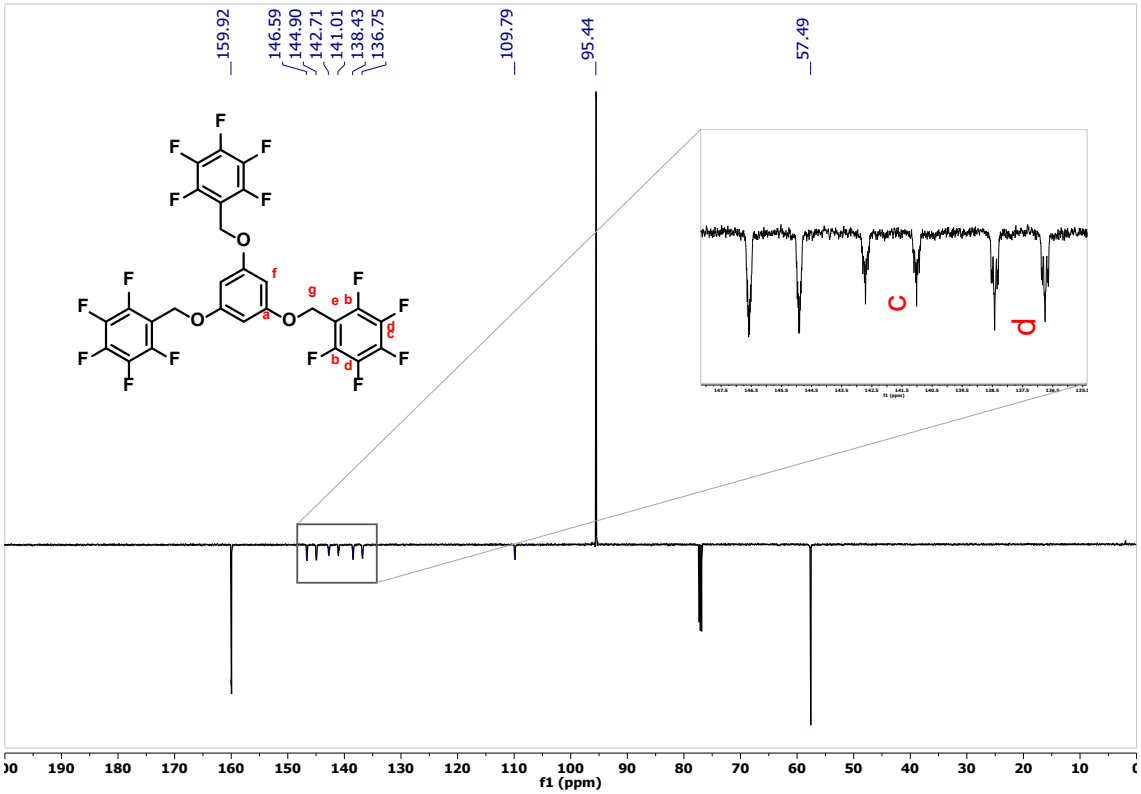

Figure S3. {^{1}H}-^{13}C NMR spectrum ($CDCl_3$, 150 MHz) of **3PFB**.

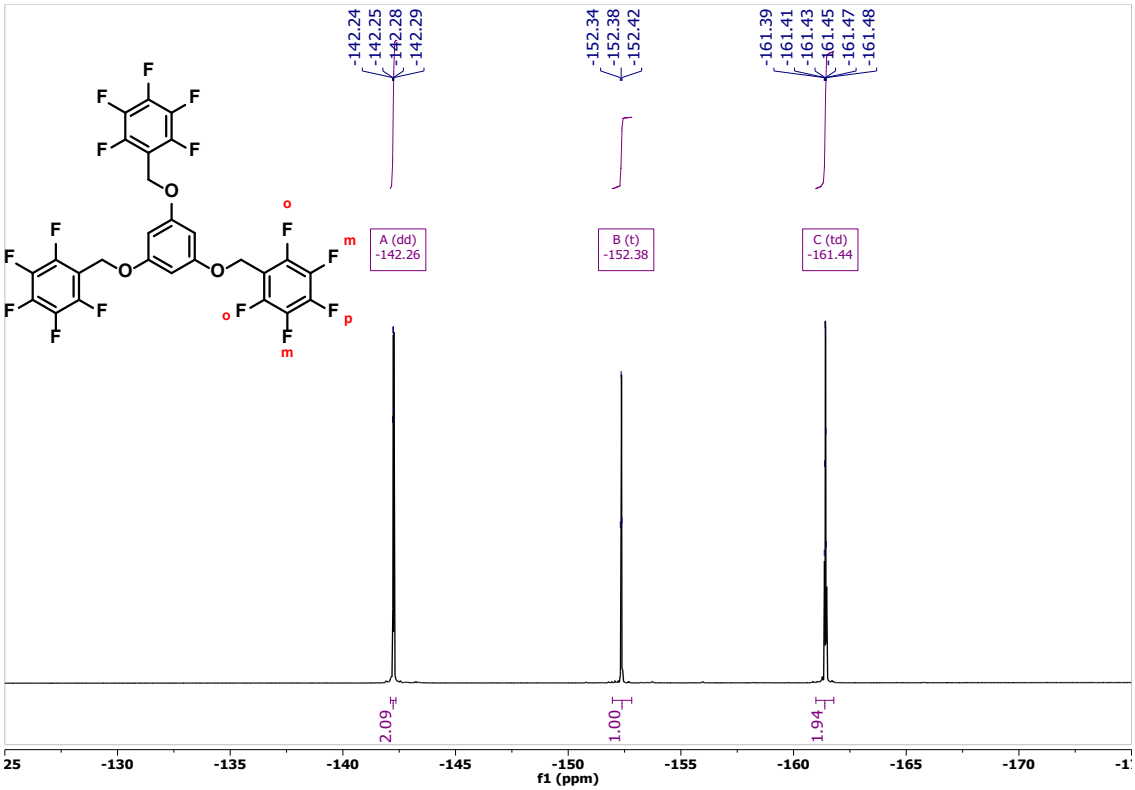

Figure S4. ^{19}F NMR spectrum ($CDCl_3$, 564 MHz) of **3PFB**.

PFTR

The pFTR linker (111 mg, 167 µmol, 1.00 eq) was dissolved in ACN (25 mL), purged with Argon for 10 min and split into five solutions of 5 mL each. Separately, solutions of thiol (10.0 µmol, 0.30 eq to 100 µmol, 3.00 eq) and TBAOH (10.0 µL, 10.0 µmol, 0.30 eq to, 100 µL, 100 µmol, 3.00 eq) in ACN (5 mL) were prepared. The thiolate solutions were subsequently added to the linker solutions and the mixtures were stirred at 50 °C for 12 h.

The reactions were carried out in acetonitrile (ACN) as it is an excellent solvent for conducting PFTR (*i.e.* polar and aprotic), and the CL reaction of the CL probe in ACN with TBAF is a well-established system with reported quantum yields.

^{19}F NMR ($CDCl_3$): δ = -132.23 (m, 6F, *ortho*), -144.95 (m, 6F, *meta*) ppm.

Chlorinated Schaap's dioxetane

Schaap's dioxetane bearing a chlorine substitution in *ortho*-position has been synthesised according to literature.[1]

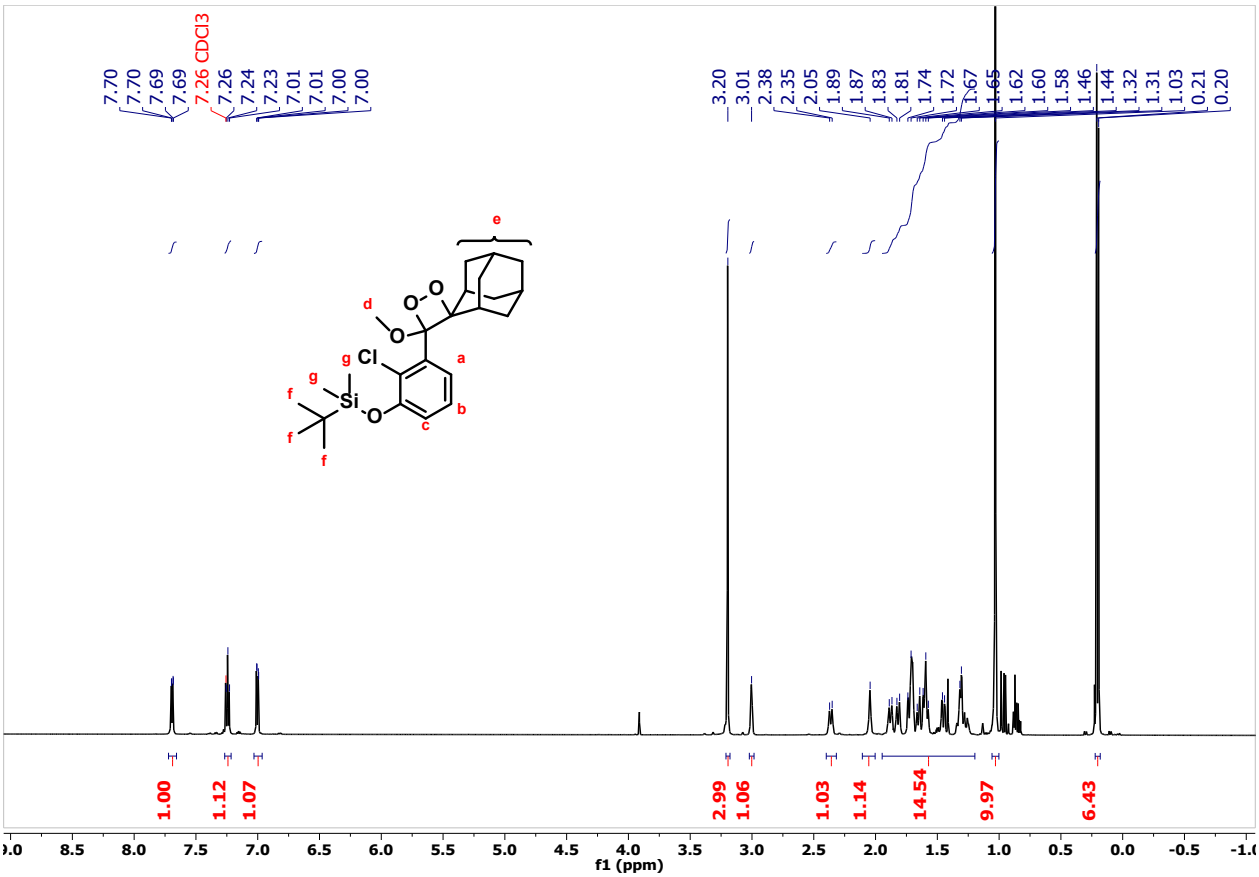

Figure S5. ^{1}H NMR spectrum ($CDCl_3$, 600 MHz) of the CL probe 'Schaap's dioxetane

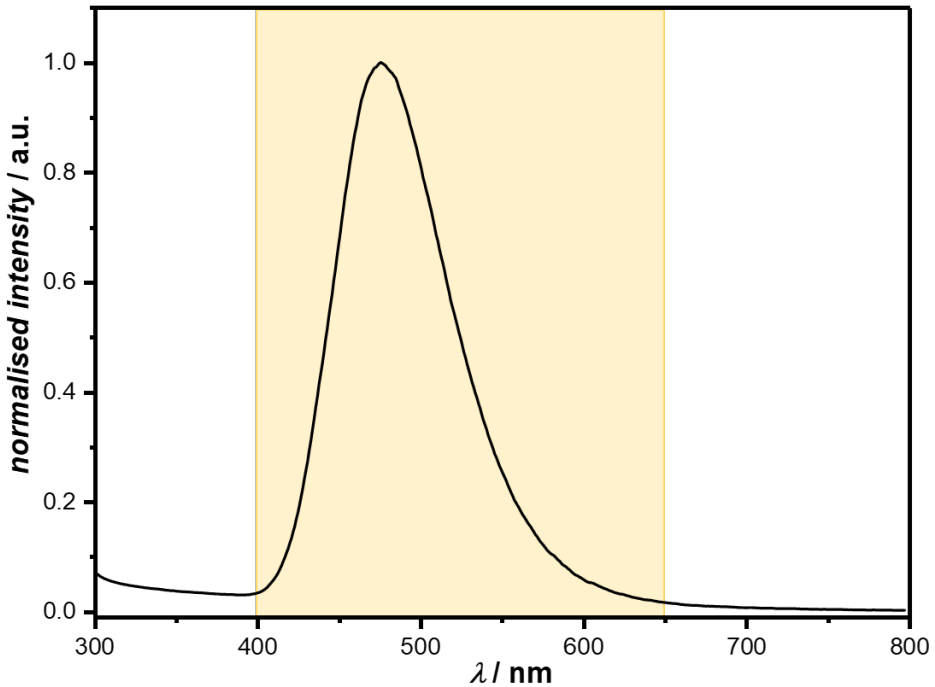

Figure S6. CL mission spectrum of the CL probe in acetonitrile. The yellow box highlights the wavelength regime that was recorded and integrated.

IV. Time-dependant Emission

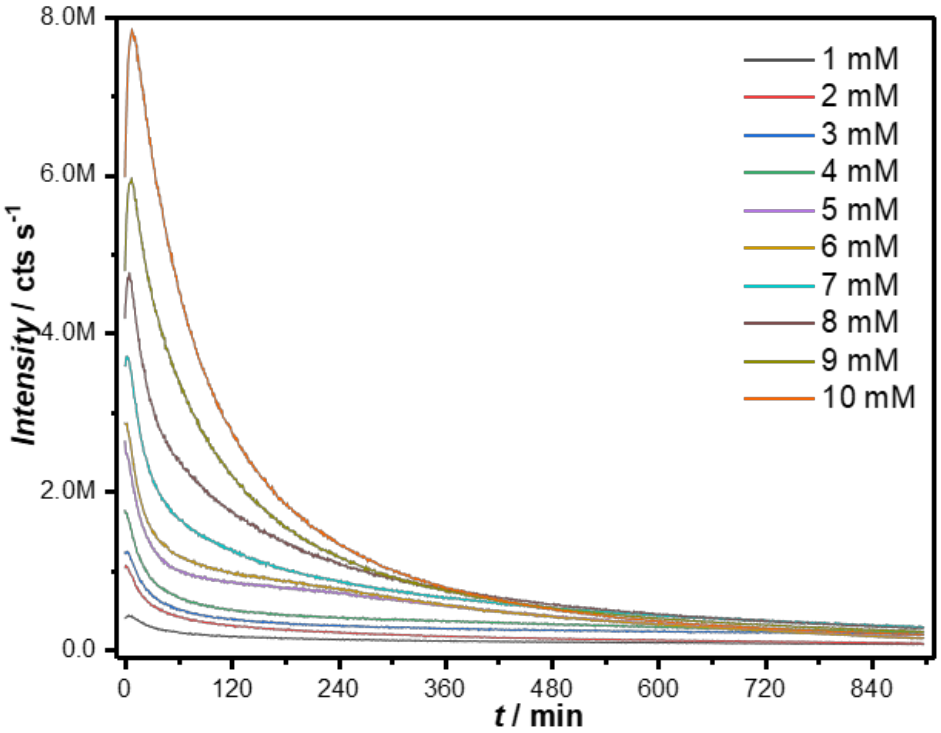

Figure S7. Time-dependant CL intensity of TBAF at various concentrations over the course of 15 h.

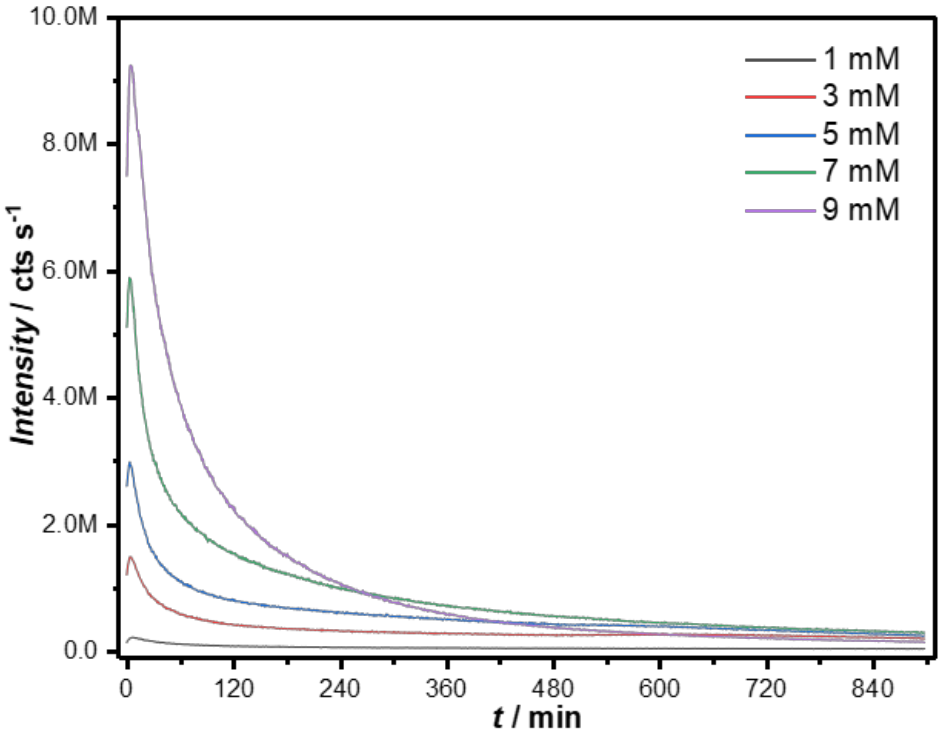

Figure S8. Time-dependant CL intensity after PFTR of AT and 3PFB at various concentrations over the course of 15 h.

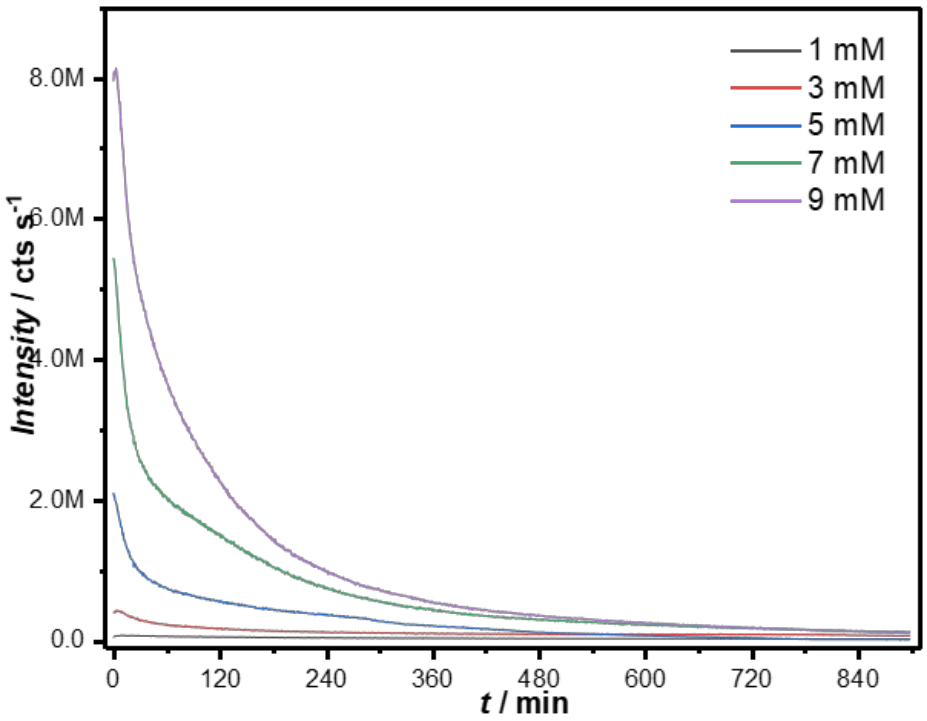

Figure S9. Time-dependant CL intensity after PFTR of mTrEGT and 3PFB at various concentrations over the course of 15 h.

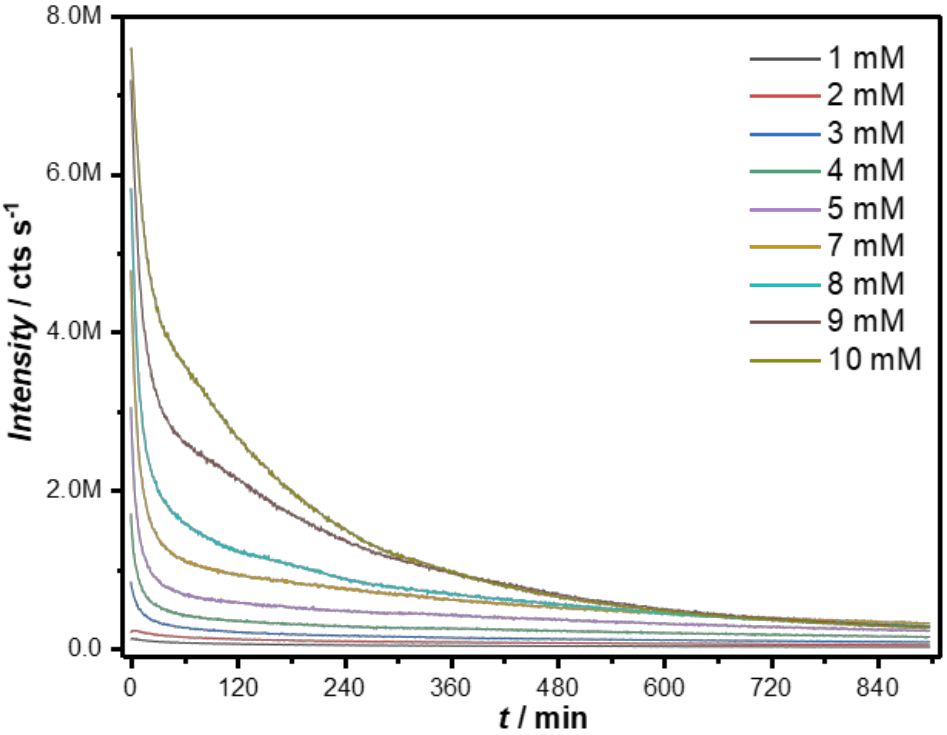

Figure S10. Time-dependant CL intensity after PFTR of BT and 3PFB at various concentrations over the course of 15 h.

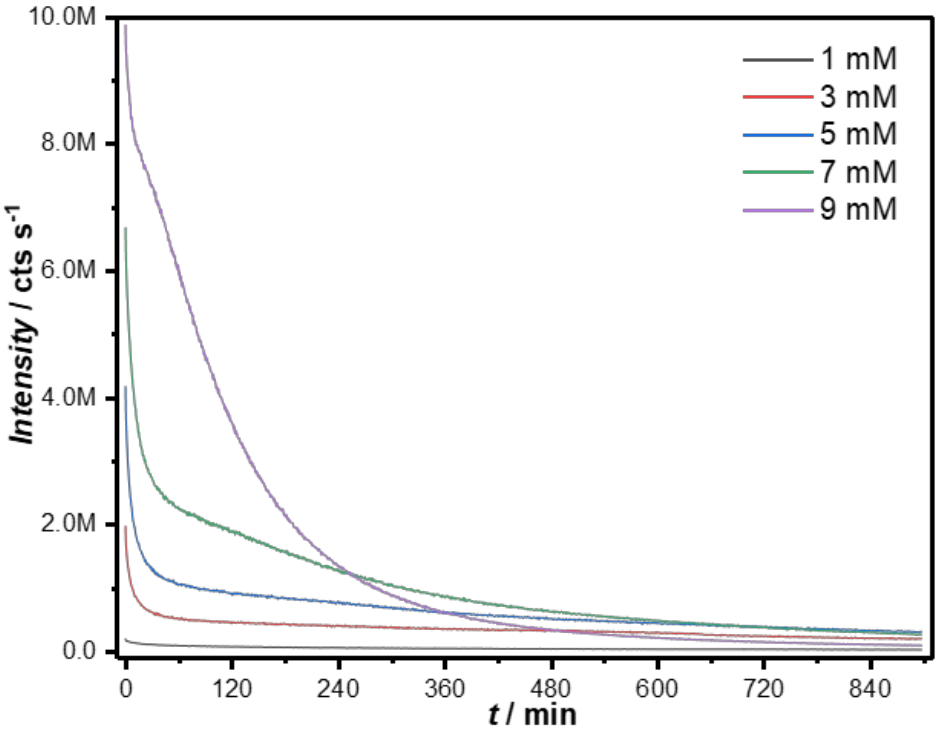

Figure S11. Time-dependant CL intensity after PFTR of PEG-SH and 3PFB at various concentrations over the course of 15 h.

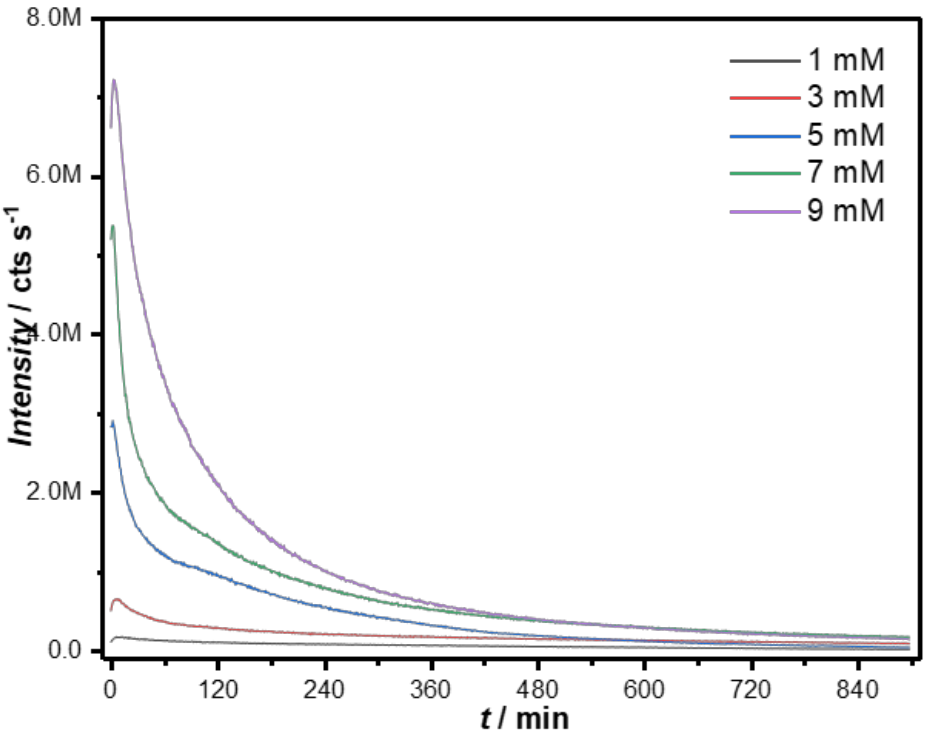

Figure S12. Time-dependant CL intensity after PFTR of BDT and 3PFB at various concentrations over the course of 15 h.

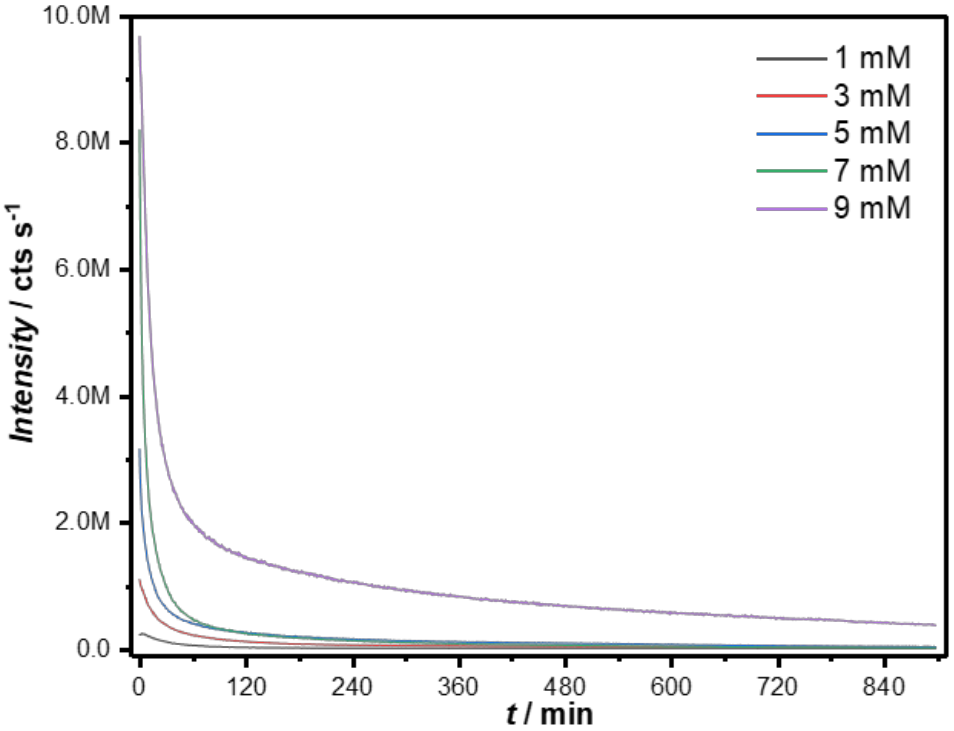

Figure S13. Time-dependant CL intensity after PFTR of DODT and 3PFB at various concentrations over the course of 15 h.

V. Anion Testing

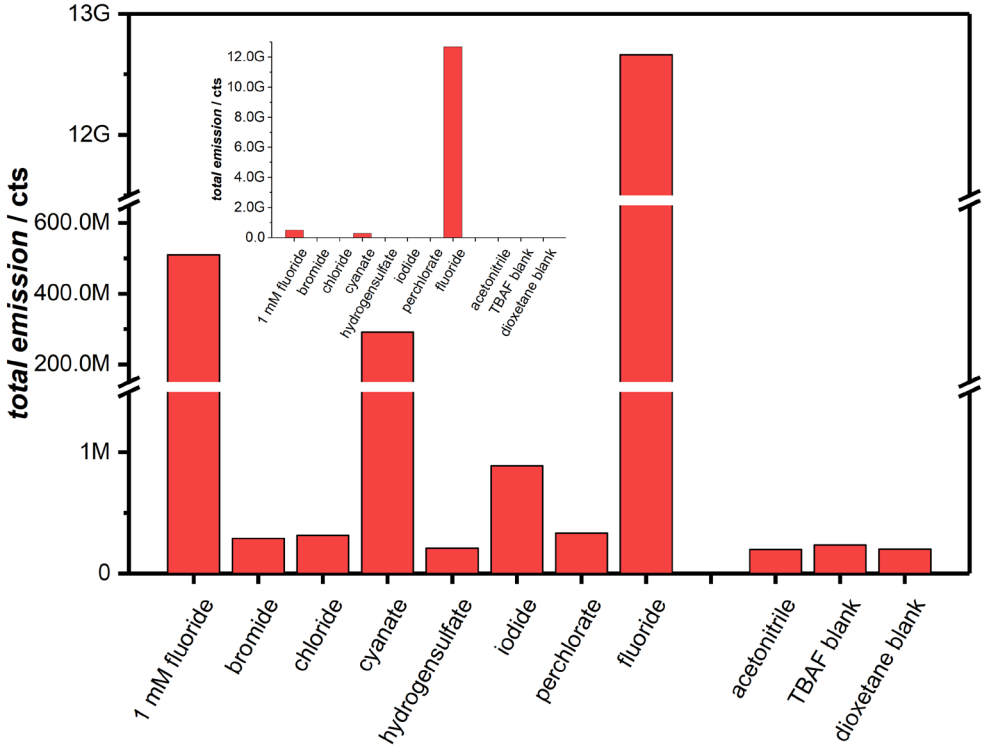

Figure S14. Total integrated CL emission of 10 mM solutions TBA bromide, chloride, cyanate, hydrogensulfate, iodide, perchlorate and fluoride as well as a 1 mM solution of TBAF. After 2 h, cyanate shows only 2.3% of the integrated CL intensity compared to equimolar amounts of fluoride and only 57% of integrated CL compared to 0.1 equivalents of fluoride. Integrated CL intensity for the other investigated anions lies between 16 and 70 ppm.

The reason for the good selectivity of fluoride compared to other anions is the high affinity of fluoride towards silicon (binding energy of Si-F is 595 kJ mol^{-1}, compared to Si-Br 329, Si-Cl 398, Si-I 234 and Si-O 444 kJ mol^{-1}) as well as its smaller radius of 133 pm compared to cyanate 159 pm, chloride 181 pm, bromide 196 pm, iodide 220 pm, perchlorate 240 pm and hydrogensulfate 258 pm.

VI. Calculation of Conversion

Conversion of PFTR was calculated from ^{19}F NMR by comparing the ratios of parent ortho- (o), meta- (m) as well as para-fluoro (p) resonances with the ortho' (o')- and meta'-fluoro (m') resonances of the PFTR product, as shown in **Fig. S7**, according to **equation S1**.

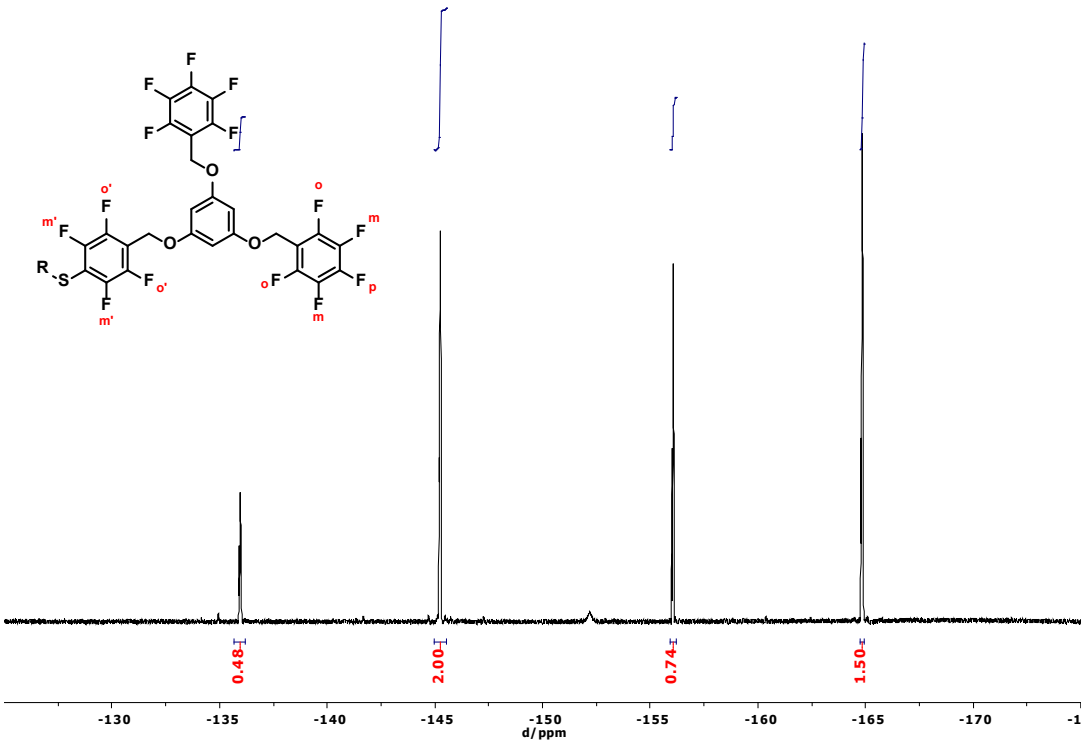

Figure S15. ^{19}F NMR spectrum (ACN-d_3, 564 MHz) of **3PFB** after approx. 24% conversion in a PFTR.

$$conversion\ (c) = \frac{m'}{m' + m} = \frac{0.48}{0.48 + 1.50} \approx 0.242 \triangleq 24.2\%$$

Equation S1. Calculation of conversion from ^{19}F NMR without any hydroxide substitution occurring.

As NMR commonly exhibits errors of up to 5%, error propagation was performed according to **equation S2**, where *∂/∂c* is the derivation of the conversion (refer to **equation S1**) and *Δ* is the error of the according integral:

$$Error = \left|\frac{\partial m'}{\partial c}\right| * \Delta\mathrm{m}' + \left|\frac{\partial m}{\partial c}\right| * \Delta\mathrm{m}$$

Equation S2. Error propagation of conversion based on ^{19}F NMR without any hydroxide substitution occurring.

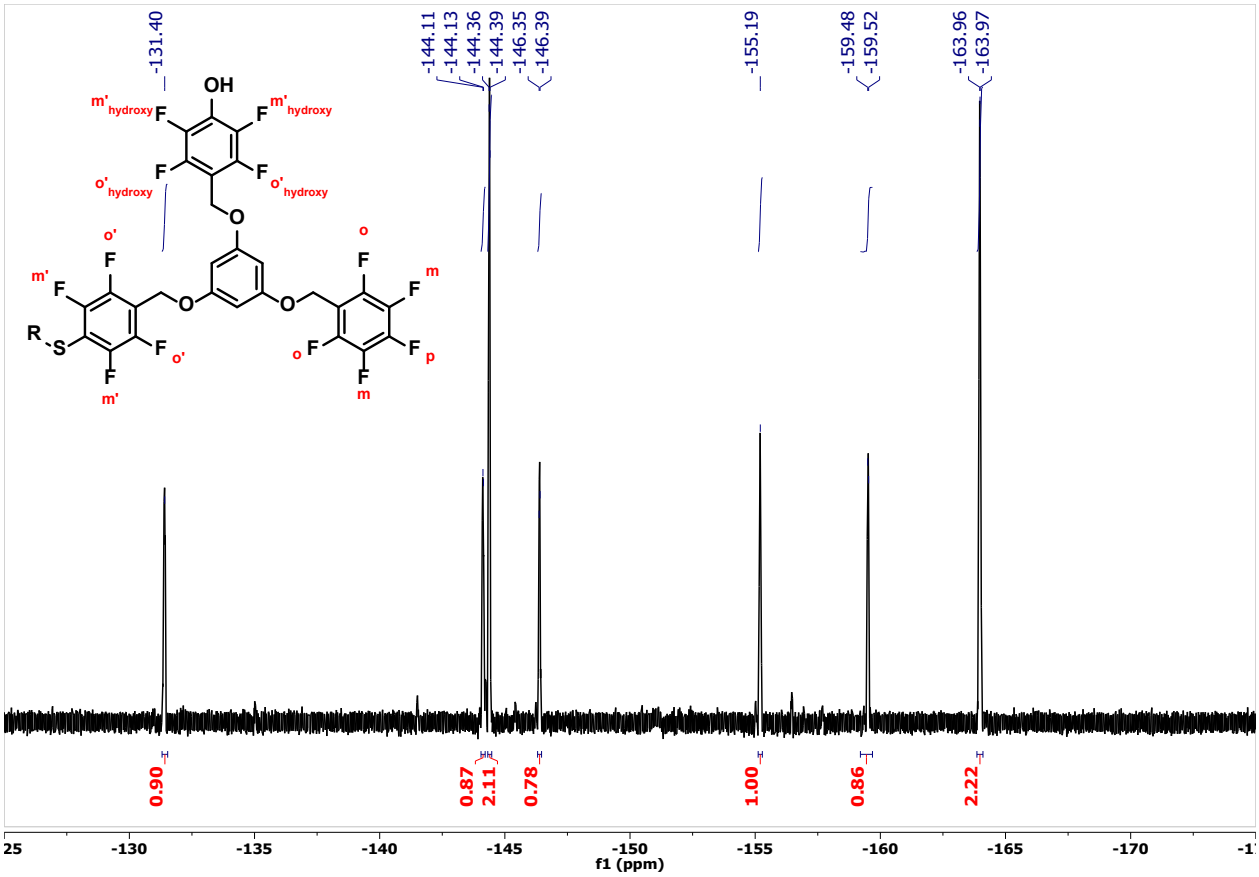

Figure S16. ^{19}F NMR spectrum (ACN-d_3, 564 MHz) of **3PFB** after approx. 23% conversion in a PFTR and 22% hydroxy substitution.

$$conversion\ (c) = \frac{m'}{m' + m + m'_{hydroxy}} = \frac{0.90}{0.90 + 2.22 + 0.86} \approx 0.226 \triangleq 22.6\%$$

Equation S3. Calculation of conversion from ^{19}F NMR with hydroxide substitution occurring.

$$Error = \left|\frac{\partial m'}{\partial c}\right| * \Delta\mathrm{m}' + \left|\frac{\partial m}{\partial c}\right| * \Delta\mathrm{m} + \left|\frac{\partial m'_{hydroxy}}{\partial c}\right| * \Delta\mathrm{m}$$

Equation S4. Error propagation of conversion based on ^{19}F NMR without any hydroxide substitution occurring.

Conversion of PFTR was furthermore calculated from LC by comparing the weighted ratios of unsubstituted as well as mono-, bis- and trisubstituted linkers, as shown in **Fig. S5**, according to **equation S3**. The conversion of **PEG-SH** was calculated from SEC in the same manner.

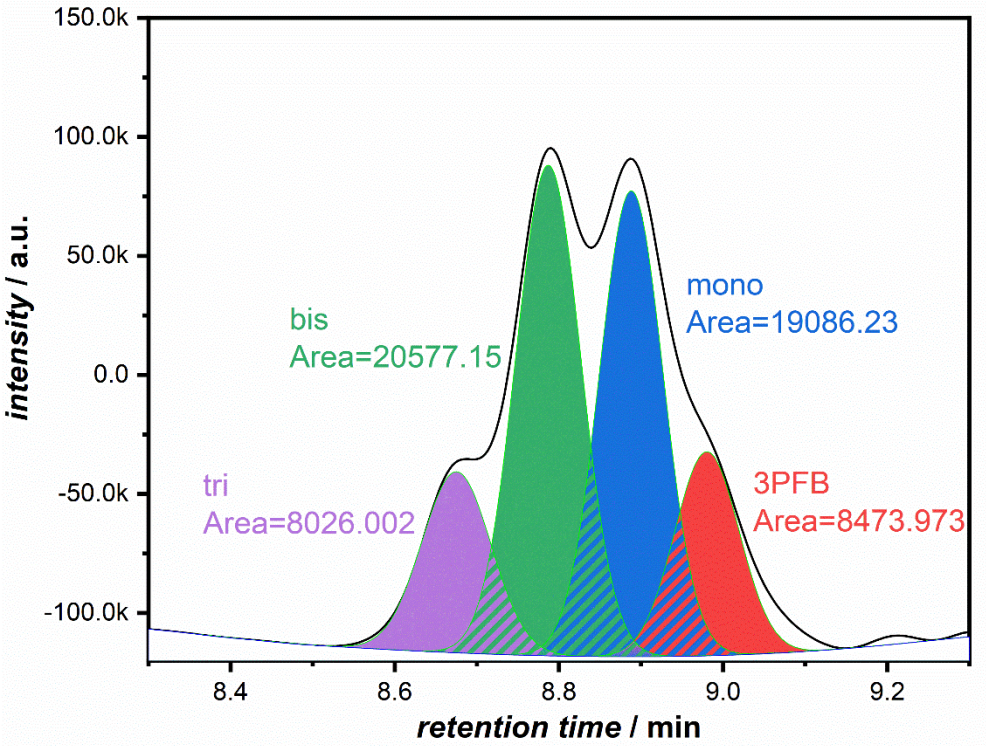

Figure S17. LC chromatogram of **3PFB** after approx. 50% conversion in a PFTR.

$$conversion\ (c) = \frac{A_{mono} + 2 * A_{bis} + 3 * A_{tri}}{3 * (A_{3PFB} + A_{mono} + A_{bis} + A_{tri})} = \frac{84{,}318.5}{168{,}490} \approx 0.500 \triangleq 50.0\%$$

Equation S3. Calculation of conversion from LCMS.

Error calculations were performed based on the difference between the deconvoluted LC trace and the original LC trace (ΔA), according to:

$$Error = \left|\frac{\partial A_{3PFB}}{\partial c}\right| * \Delta A + \left|\frac{\partial A_{mono}}{\partial c}\right| * \Delta A + \left|\frac{\partial A_{bis}}{\partial c}\right| * \Delta A + \left|\frac{\partial A_{tri}}{\partial c}\right| * \Delta A$$

VII. Linear Fits of Emission vs Conversion

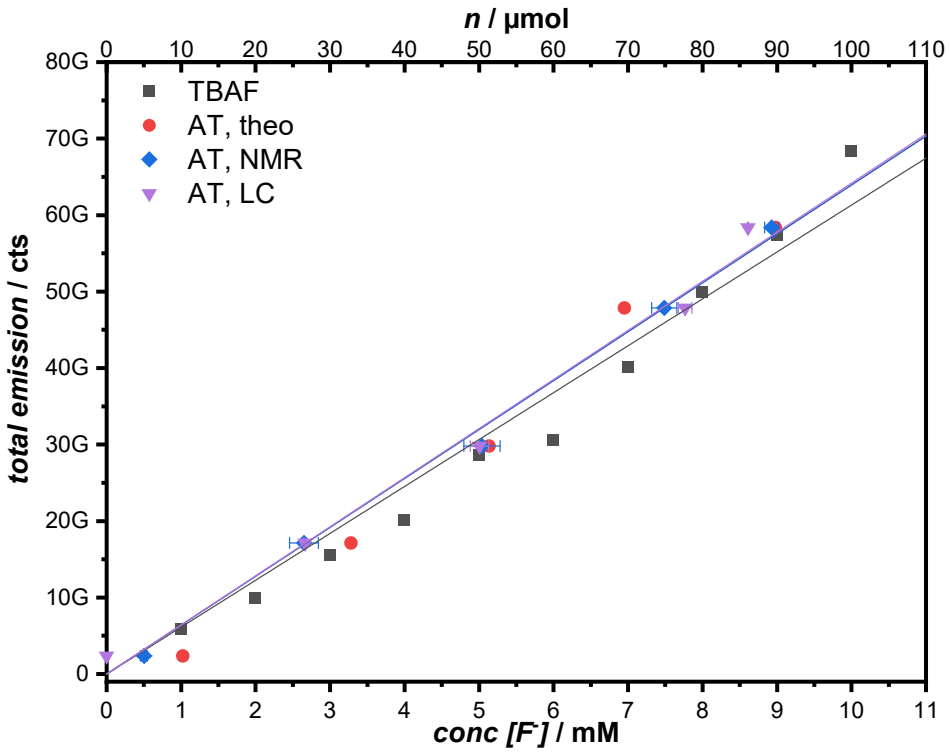

Figure S18. CL emission vs fluoride concentration for adamantyl thiol (AT) according to expected yields (red dots), ^{19}F NMR conversion (blue diamonds), and LC (purple triangles) compared to the TBAF reference (black squares).

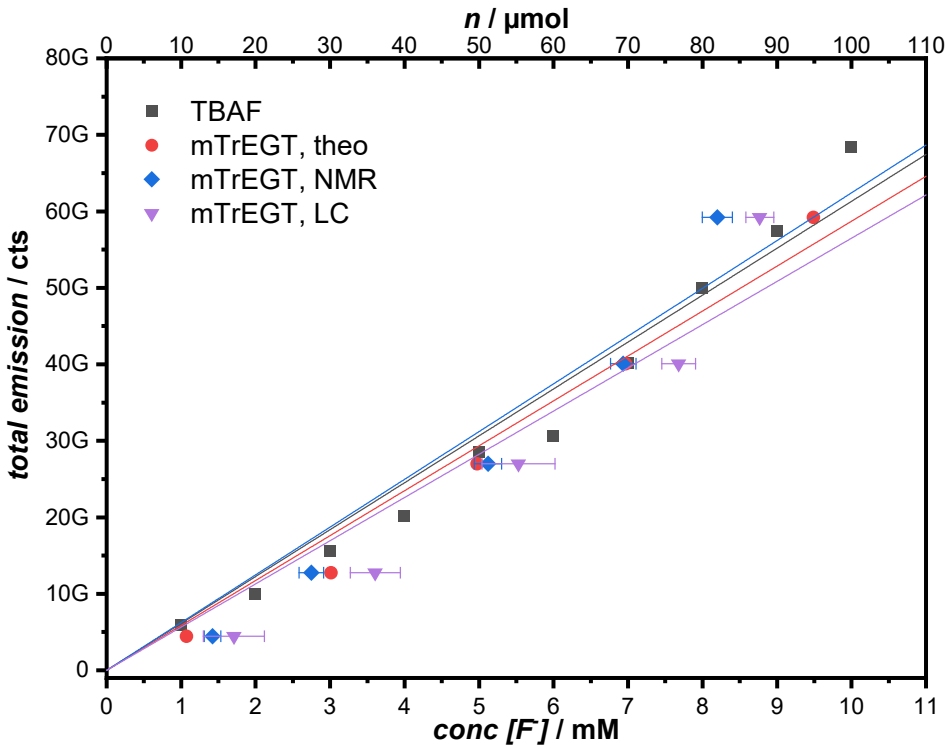

Figure S19. CL emission vs fluoride concentration for methoxy triethylene glycol thiol (mTrEGT) according to expected yields (red dots), ^{19}F NMR conversion (blue diamonds), and LC (purple triangles) compared to the TBAF reference (black squares).

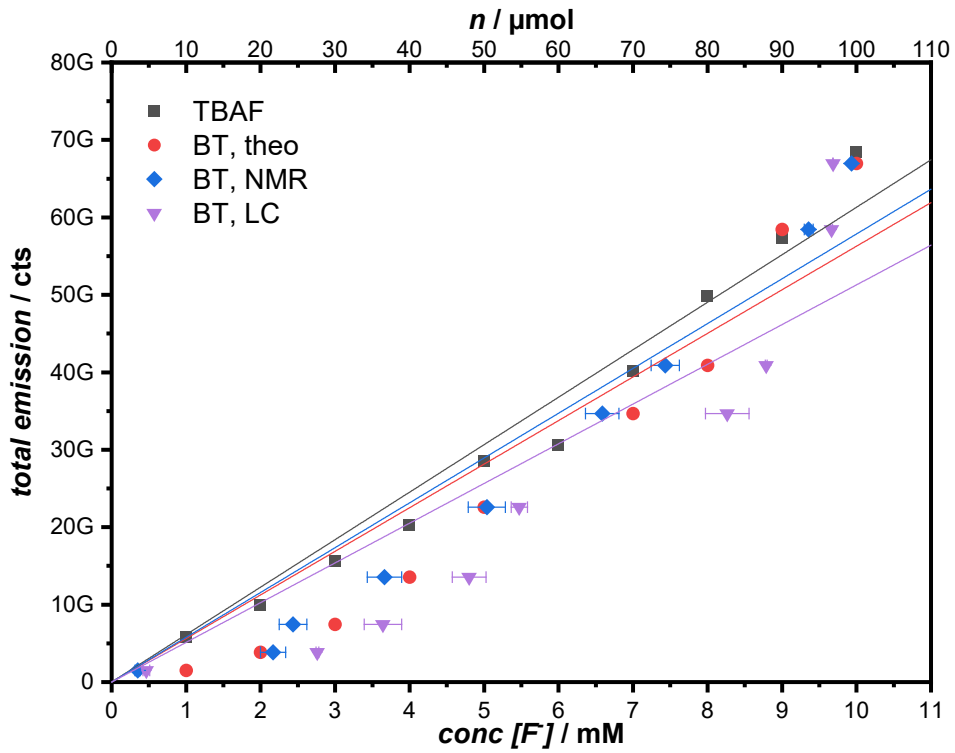

Figure S20. CL emission vs fluoride concentration for benzyl thiol (BT) according to expected yields (red dots), ^{19}F NMR conversion (blue diamonds), and LC (purple triangles) compared to the TBAF reference (black squares).

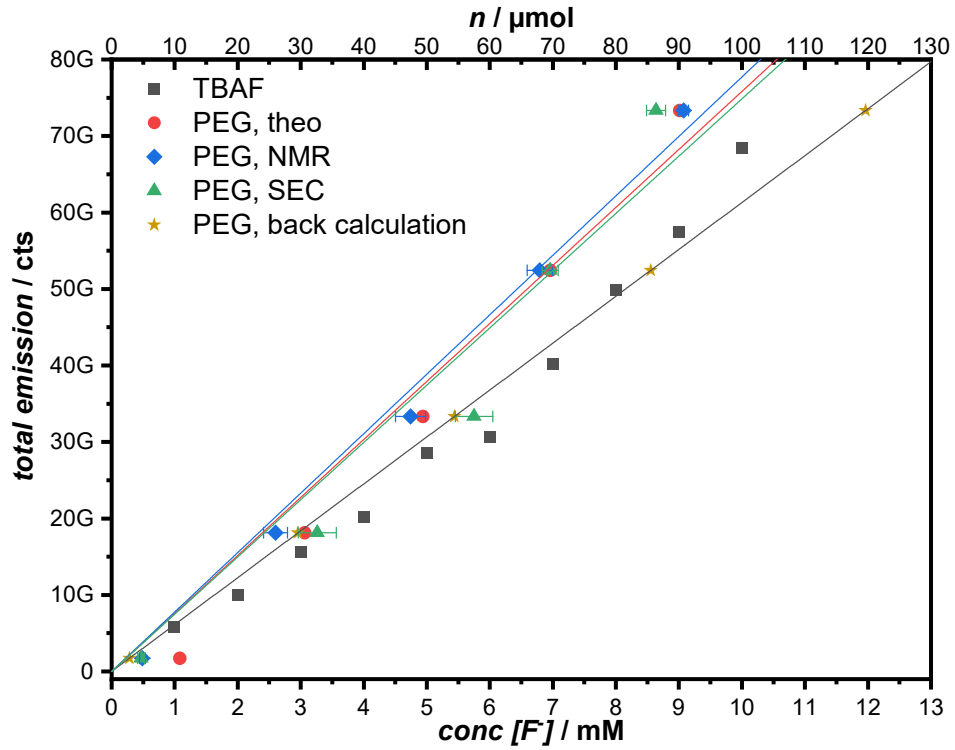

Figure S21. CL emission vs fluoride concentration for poly(ethylene glycol) thiol (PEG-SH) according to expected yields (red dots), ^{19}F NMR conversion (blue diamonds), and LC (purple triangles) compared to the TBAF reference (black squares). The golden stars depict the concentration of fluoride as calculated from the CL emission.

VIII. Supplementary Network Data

The PFTR networks describes in the manuscript were subjected to ^{19}F NMR and SEC analysis in order to determine if any soluble fraction was present.

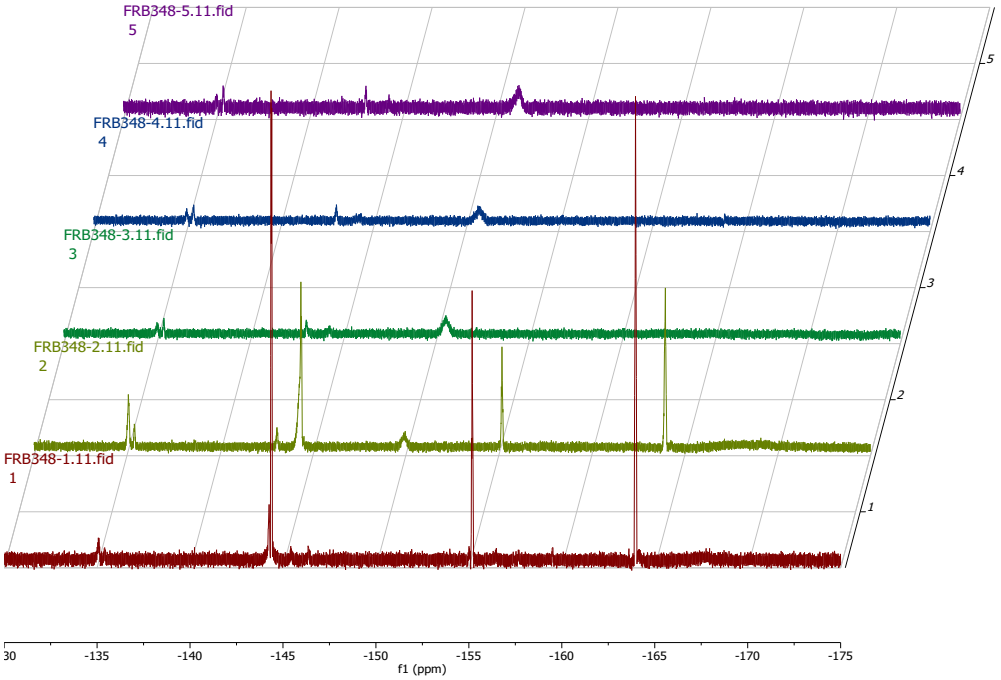

Figure S22. ^{19}F NMR spectrum (ACN-d_3, 564 MHz) of the supernatant solutions after network formation employing BDT. Traces 3 to 5 do not show any significant amount of PFB resonances.

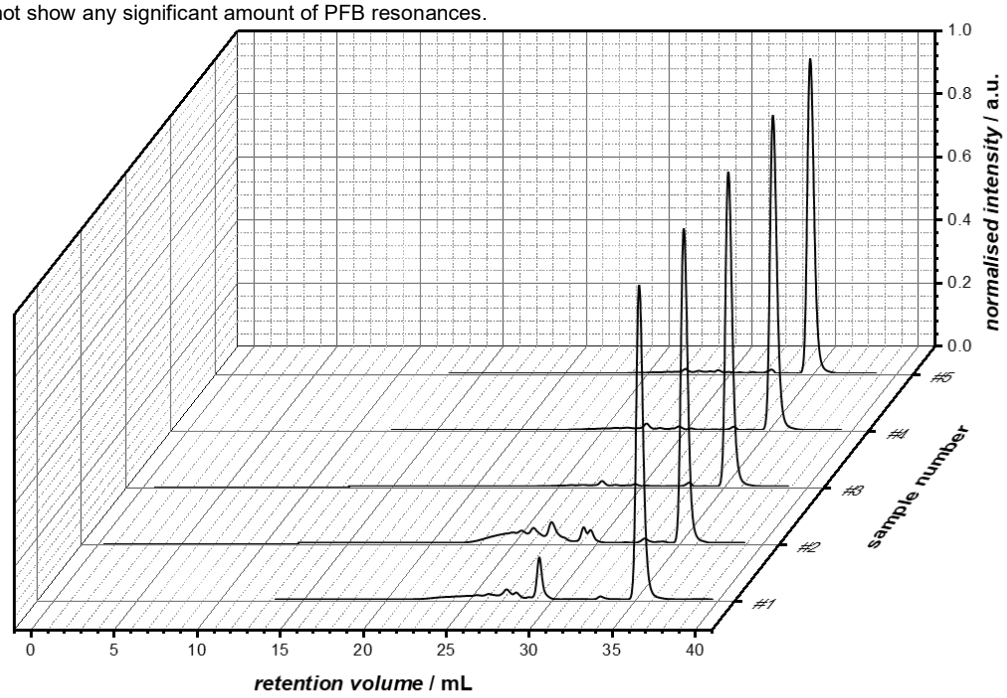

Figure S23. SEC spectra of the supernatant solutions after network formation employing BDT. Toluene was added to the SEC samples (1 mg mL^{-1}, @35.35 mL retention volume) in order to provide a reference. Traces 3 to 5 do not show any significant amount of soluble fractions.

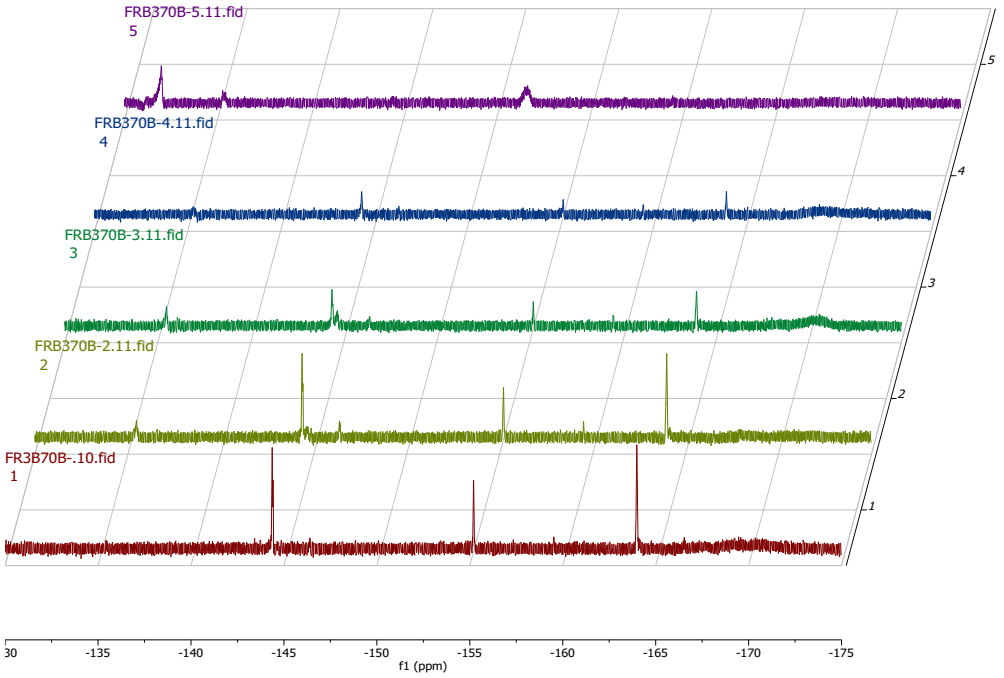

Figure S24. ^{19}F NMR spectrum (ACN-d_3, 564 MHz) of the supernatant solutions after network formation employing DODT. Only trace 5 does not show any significant amount of PFB resonances.

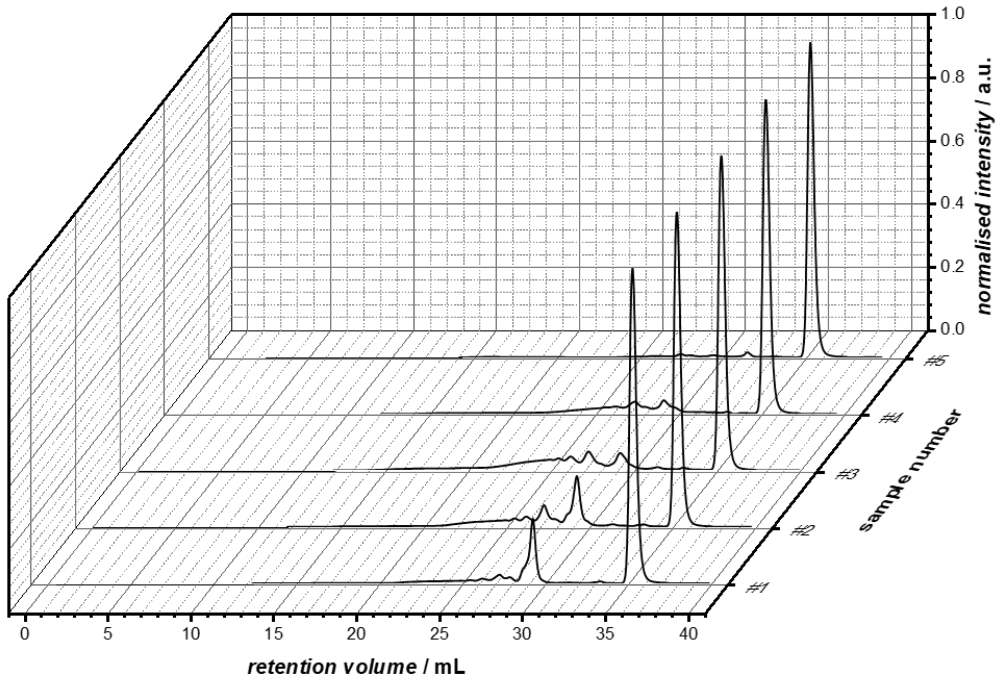

Figure S25. SEC spectra of the supernatant solutions after network formation employing DODT. Toluene was added to the SEC samples (1 mg mL^{-1}, @35.35 mL retention volume) in order to provide a reference. Only trace 5 does not show any significant amount of soluble fractions.

IX. Hydroxy-Substitution of *p*-Fluorine

In some cases, the employed base TBAOH partially undergoes nucleophilic substitution with the 3PFB linker rather than deprotonate the thiol. In these cases, additional resonances at around 146.3 and 159.5 ppm appear in the ^{19}F NMR spectrum (refer to Figure S16). While the hydroxy-substitution also releases one equivalent of fluoride per reaction, the fluorine will subsequently deprotonate a thiol and form HF. Due to similar pKa values of the thiol and HF, the thiol and the fluoride are in an equilibrium with HF and the thiolate. However, as the thiolate is subsequently reacted with the 3PFB linker, the equilibrium is eventually completely shifted to HF and the thiolate. On the one hand, the deprotonation of thiols *via* fluoride ensures that full conversion of thiols can still be achieved, on the other hand the formed HF does not trigger significant amounts of CL und thus, does not falsify the PFTR read-out. Refer to Scheme S1 for more information.

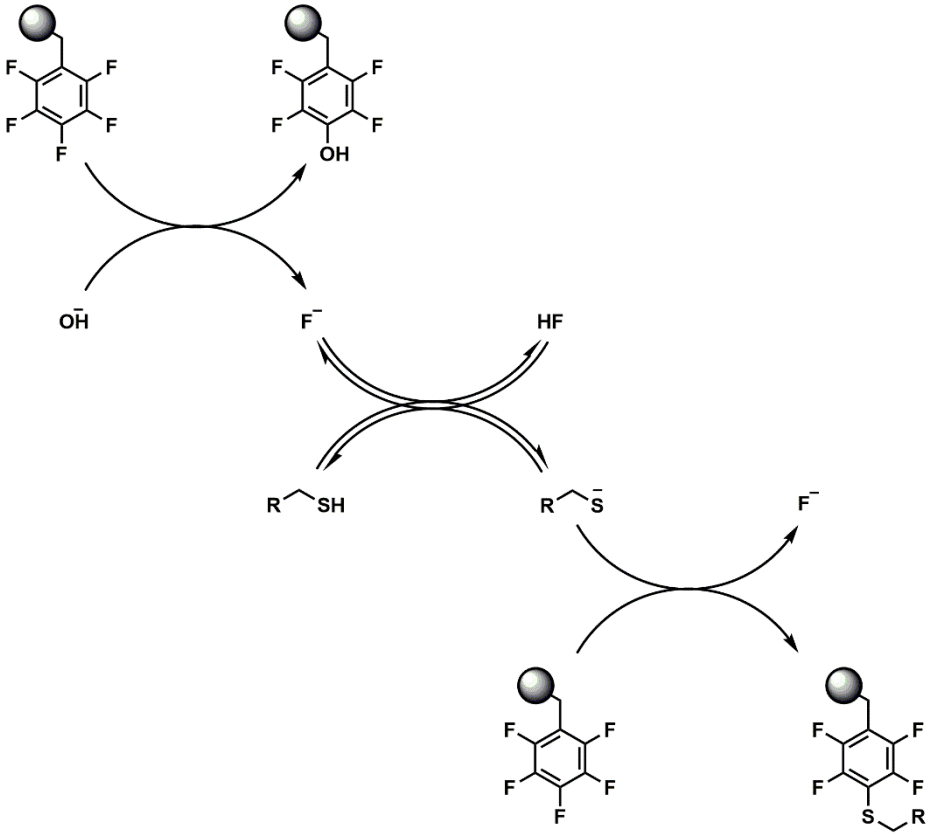

Scheme S1. A hydroxide reacts with the 3PFB linker and releases a fluoride. The pK_a of HF-fluoride acid-base pair is low enough to allow deprotonation of a thiol, which can subsequenly undergo PFTR and release another fluoride ion. Contrary to a free fluoride, the HF formed upon deprotonation of the thiol will not trigger significant chemiluminescent. Thus, the CL read-out obtained only refers to thiol substitution, but not hydroxy substitution.

X. References

[1] N. Hananya, A. Eldar Boock, C. R. Bauer, R. Satchi-Fainaro, D. Shabat, *J. Am. Chem. Soc.* **2016**, *138*, 13438–13446.